Materials Research Bulletin 48 (2013) 5026–5032

Contents lists available at SciVerse ScienceDirect

Materials Research Bulletin

journal homepage: www.elsevier.com/locate/matresbu

Elastic modulus of rat whiskers—A key biomaterial in the rat whisker sensory system

Qianhua Kan [a], Ramesh Rajan [b], Jing Fu [c], Guozheng Kang [a], Wenyi Yan [c,*]

[a] School of Mechanics and Engineering, Southwest Jiaotong University, Chengdu 610031, China
[b] Department of Physiology, Monash University, Clayton, VIC 3800, Australia
[c] Department of Mechanical & Aerospace Engineering, Monash University, Clayton, VIC 3800, Australia

ARTICLE INFO

Article history:
Received 17 March 2013
Received in revised form 29 April 2013
Accepted 30 April 2013
Available online 9 May 2013

Keywords:
A. Organic compounds
D. Elastic properties
D. Mechanical properties

ABSTRACT

Nanoindentation tests were carried out to measure the elastic modulus of rat whisker, which is used as a high-acuity sensor for exploring the world and discriminating object distance, size and surface texture. The measured load–depth curves show that the biomaterial of rat whisker exhibits obvious visco-elastic characteristic, such as load relaxation and displacement creeping. The measured indentation modulus of rat whiskers decreases with indentation depth at the same location. The mean value of the measured indentation moduli of 24 major whiskers varies from 0.33 GPa to 4.92 GPa. The elastic modulus is independent of the freshness of the whisker sample. It is also found that the length and diameter of whiskers have no direct relationship to the indentation modulus at the base. Based on the measured elastic modulus, the bending stiffness at the base of a whisker is predicted in the range of 0.58–134.79 mN mm^2 and the rotational stiffness at the middle of a whisker is within 0.06–10.93 mN mm/rad. These results can be used to study the mechanical behavior of the rat whisker sensor system.

1. Introduction

The rat whisker system is an important research model in neuroscience and in bionics for the study of the sense of touch and object discrimination [1–4]. During a typical exploration, rats sweep their whiskers against and over an object to detect information such as position, shape and surface texture of the object [1]. Rat whiskers have no receptors along their length [5] and all the information gained about an object must be transmitted along the whisker length to sensory neurons at the whisker base. This transmission of mechanosensory information will depend on properties of the whisker, specifically the bending stiffness of the whisker [6] and whisker resonance [7,8]. To understand this highly sensitive biosensory system, we need to elucidate its biomechanics so as to understand the interaction between whiskers and objects. From the mechanics point of view, knowing the elastic modulus of rat whisker is a prerequisite in the biomechanics study. This property has been investigated using different methods, summarized in Table 1, and it has been shown that the elastic modulus of rat whisker varies from 1.4 GPa to 7.8 GPa [3,7–10,15], depending on the adopted mechanical models and test methods.

Recently, the technique of nanoindentation has become widely used for measuring the elastic modulus of biomaterials such as human dentin [11], porcine sclera [12], trabecular bone [13], and wing membrane of dragonfly [14]. Nanoindentation testing produces a force–displacement curve and enables the determination of hardness and elastic modulus. The test does not require large and well-arranged specimens because the indentation zone is localized. Previous nanoindentation tests [15] show that the elastic modulus of whisker B1 (the first whisker in row B of the five rows, A–E, of the rat's face whiskers) is 3.1–3.9 GPa, but the study was only performed on a single sample whisker B1. The objective of current study is to systematically measure the elastic moduli of 24 major rat whiskers by carrying out nanoindentation testing. We first describe the details of the whisker samples and experimental methods in Section 2, then present and discuss the indentation modulus of 24 whiskers in Section 3, and finally present conclusions in Section 4. Based on the measured elastic modulus, the mechanical properties of a rat whisker, such as the bending and the rotational stiffness, can be predicted and they can be applied to study the mechanical behavior of a rat whisker sensor system or a biomimetic one.

2. Material and experimental method

2.1. Sample preparation

Whisker samples were obtained from a 3-month old (adult) female Sprague-Dawley rat. All procedures to deal with the rat had been approved by Monash University Animal Welfare Committee.

* Corresponding author. Tel.: +61 399020113; fax: +61 399051825.
E-mail address: wenyi.yan@monash.edu (W. Yan).

0025-5408/$ – see front matter © 2013 Elsevier Ltd. All rights reserved.
http://dx.doi.org/10.1016/j.materresbull.2013.04.070

Table 1
Summary of indentation modulus of rat whisker reported in literature.

E (GPa)	Method	Whisker samples	References
1.4–6.25	Estimated from deflection tests	β, γ, A1, E2, B2, E3, C3	[3]
3.02–3.68	Estimated from bending resonant experiment	24 whiskers	[7]
7.8	Estimated from bending resonant experiment	10 whiskers	[8]
7.36	Estimated from bending tests	14 whiskers	[9]
2.9–3.96	Uniaxial tensile test	22 whiskers	[10]
3.1–3.9	Nanoindentation	B1	[15]

24 major rat whiskers on one side of the rat's snout, consisting of an arc of whiskers named as α, β, γ, and δ whiskers, and five rows, each with 4 whiskers (A1–A4, B1–B4, ..., E1–E4), were studied. Each whisker was grasped at the base by a fine forceps and pulled out from the rat's face. To eliminate the influence of clamping by the tweezer on whisker material, nanoindentation tests were carried out at 3–4 mm away from the base. The samples were cleaned by alcohol and flatted on glass slides for nanoindentation test.

2.2. Nanoindentation method

Nanoindentation measurements were performed by using a nano-mechanical testing system (TI750, HYSTRON, USA), which has a maximum indentation depth of 5 μm. A diamond Berkovich pyramidal indenter with a tip radius of 50 nm was used in all measurements. Before and after each set of indentations, the area was imaged at high resolution using statistical parametric mapping techniques at a constant load of 0.5 μN in a closed-loop profilometer. These images were exploited to identify a smooth surface and determine the precise location of the Berkovich indenter tip on the target area. Fig. 1 shows the morphology of rat whisker C2 at different scales. Fig. 1a is the entire whisker, which is visible to the naked eye, Fig. 1b is the tip of the whisker, and Fig. 1c shows the whisker around its base. All indentation tests were carried out in the base area, at 3–4 mm away from the base.

The method of surface preparation can affect mechanical properties because surface roughness can have a significant impact on the measurement of modulus using nanoindentation methods [16]. Nanoindentation is carried out within a very small zone; within this zone, the surface of the rat whisker is actually quite smooth although it has a round shape at the macroscopic scale, as shown in Fig. 1d. Detailed surface measurement showed that all tested surfaces had an average roughness about 21.2 nm. It has been suggested [17] that indentation depth should be chosen so that the surface roughness is less than 10% of the total indentation depth; for the average roughness of our test areas, indentation depth should be larger than 212 nm.

In cross-section, rat whiskers consist of three layers – the external cuticle, the middle cortex and the internal medulla [10]. The cuticle makes up about 15% of the total diameter at the whisker base [10,18]; the thickness of this layer for all tested whiskers can be calculated to be about 13–30 μm according to the

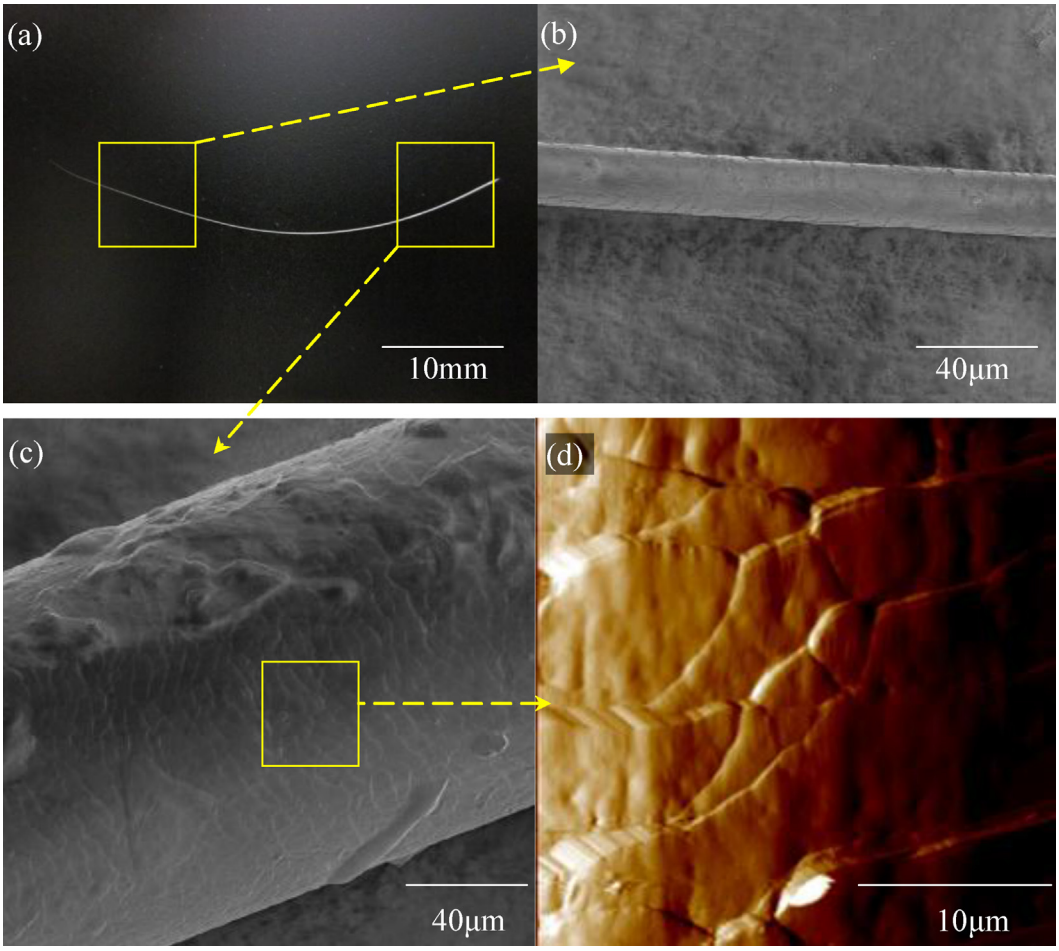

Fig. 1. The morphology of rat whisker sample C2: (a) the whole whisker photographed by a camera; (b) the whisker tip from SEM (1000×); (c) the whisker base from SEM (1000×); and (d) a local image of the base obtained from indentation instrument by SPM with a scan size of 30 μm × 30 μm.

Table 2
Measured geometrical characterization and mean indentation modulus of the 24 major whiskers (mean value ± standard deviation).

Whiskers	L (mm)	D_{base} (μm)	E_r (GPa)	$M(L)$ (mN mm^2)	$K(L/2)$ (mN mm/rad)
α	68 ± 2	178.7 ± 16.7	1.09 ± 0.2	45.88	2.02
β	58 ± 2	199.0 ± 27.8	1.40 ± 0.41	90.64	4.69
γ	33 ± 2	191.1 ± 4.3	0.67 ± 0.17	36.87	3.35
δ	34 ± 2	181.3 ± 15.0	0.33 ± 0.08	14.71	1.30
A1	41 ± 2	126.7 ± 0.6	3.06 ± 0.38	32.60	2.39
A2	31 ± 2	109.7 ± 15.0	0.097 ± 0.032	0.58	0.06
A3	37 ± 2	111.7 ± 5.1	0.64 ± 0.11	4.11	0.33
A4	32 ± 2	87.3 ± 2.5	4.70 ± 0.60	11.30	1.06
B1	39 ± 2	140.2 ± 2.5	0.45 ± 0.12	7.17	0.55
B2	42 ± 2	126.0 ± 6.0	1.35 ± 0.42	14.05	1.00
B3	27 ± 2	95.3 ± 4.2	2.27 ± 0.40	7.74	0.86
B4	19 ± 2	101.7 ± 5.0	2.46 ± 0.31	10.87	1.72
C1	37 ± 2	158.7 ± 2.5	0.58 ± 0.16	15.18	1.23
C2	38 ± 2	144.7 ± 2.5	1.33 ± 0.18	24.07	1.90
C3	36 ± 2	123.3 ± 2.3	1.71 ± 0.32	16.32	1.36
C4	24 ± 2	84.0 ± 2.0	2.35 ± 0.41	4.83	0.60
D1	64 ± 2	170.7 ± 2.1	1.53 ± 0.39	53.64	2.51
D2	38 ± 2	155.0 ± 1.7	4.92 ± 0.58	117.60	9.28
D3	34 ± 2	116.3 ± 4.0	1.02 ± 0.19	7.70	0.68
D4	20 ± 2	92.0 ± 2.6	2.37 ± 0.31	7.02	1.05
E1	37 ± 2	189.3 ± 3.8	2.54 ± 0.40	134.79	10.93
E2	46 ± 2	166.3 ± 4.0	2.61 ± 0.64	82.50	5.38
E3	35 ± 2	146.0 ± 6.9	0.79 ± 0.15	14.81	1.27
E4	23 ± 2	99.7 ± 2.3	1.35 ± 0.31	5.51	0.72

diameter at the whisker base (see Table 2). The effect of a multi-layer structure of the materials on the indentation modulus can be neglected when indentation depth is less than 10% thickness of the tested layer [19], which implies that the indentation depth should be limited to <1.3 μm in our experiments. In addition, controlling the indentation depth can define the surface position of soft materials more accurately than controlling indentation force [20]. For these reasons, a multi-step displacement loading from 400 to 1000 nm was applied in our nanoindentation tests, as shown in Fig. 2. The trapezoidal load function can ensure that creep does not markedly affect the modulus calculation [21]. At each indentation point, six indentation tests at six different indentation depths were performed and twelve different points within a testing zone of 30 μm × 30 μm were explored. Previous studies had found that a load less than 10 μN will result in a significant error due to the effects of the sampling speed and drift of the transducer [22] so we used loads larger than 200 μN in all tests.

2.3. Indentation modulus

The Oliver–Pharr method [23] was employed to measure the elastic modulus of the rat whiskers from the load–displacement curve. When measuring the mechanical properties of microstructural features in biomaterials, a Berkovich tip is widely used to maximize the spatial resolution and allow measurement of mechanical properties at precise locations within the soft samples. This technique is particularly effective for characterizing biomaterials that are hierarchical in structure, allowing measurement of properties at small length scales that can be used to better understand or model macro-scale behavior [21].

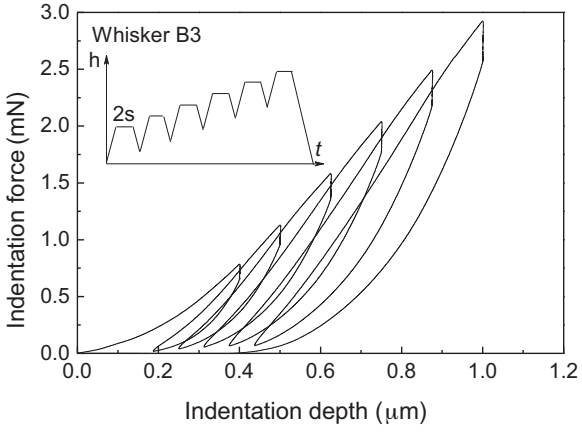

Fig. 2. Multi-step nanoindentation curves under different maximum indentation depths for whisker B3.

The indentation modulus (also called reduced modulus) E_r was calculated from the following equation:

$$E_r = \frac{S}{2}\sqrt{\frac{\pi}{A_c}} \tag{1}$$

where A_c is the projected contact area, S is the stiffness of the unloading curve and can be evaluated from unloading portion upper to 50% by a power-law function. In this indentation instrument, a plot of the calculated area as a function of contact depth is created and the TriboScan software fits the A_c versus contact depth h_c to the sixth order polynomial:

$$A_c = \sum_{n=0}^{5} C_n h_c^{2(1/2)^n} \tag{2}$$

The constants C_0, C_1, C_2, C_3, C_4 and C_5 were calibrated by nanoindentation on a fused silica. It is worth noting that the Oliver–Pharr method to estimate the contact area, Eq. (2), and the elastic modulus, Eq. (1), is only suitable for the indentations with the deformation phenomenon of "sink-in", where the surface around the indenter sinks in. If the opposite indentation deformation phenomenon of "pile-up" occurs, where the surface of the sample around the indenter being at a greater level than its surrounds, the predicted contact area will be smaller than the real one and the indentation modulus will be overestimated. Research indicates that a ratio of the reduced modulus to the yield stress less than 28 most likely results in sink-in in an indentation test [23]. This ratio is around 3.5 for rat whisker materials [10]. Therefore, the condition to apply the Oliver–Pharr method to measure the elastic modulus of rat whisker materials is satisfied.

3. Results and discussion

3.1. Geometrical characterization

As clearly visible to naked eyes, rat whiskers have a tapered shape and can be curved along their length. The geometric characteristics of the 24 major whiskers were measured by optical microscope (Nikon SMZ800, Japan). A cotton swab soaked in alcohol was used to first straighten the whiskers temporarily and it was found that the length varies from whisker to whisker, as shown in Table 2, with the possible error being less than 2 mm. We found the length to range from 19 ± 2 mm (for whisker B4) to 68 ± 2 mm (for whisker α).

Given the curvature of the whiskers in some sections, they were firstly marked every 5 mm in the attached glass slide, and then the diameter of each whisker was measured in three adjacent sections of each marked place to generate an average value that is shown in Table 2. The diameter at the base varied from whisker to whisker. The thinnest one was whisker A4 with a diameter of about 87.3 ± 2.5 μm and the thickest one is β with the diameter of about 199 ± 27.8 μm. According to Table 2, overall, whiskers α, β, γ, δ and the first one in each row had the largest lengths and diameter; whiskers at the opposite end of each row, namely A4, B4, C4, D4 and E4, had a smaller length and diameter.

The tapered shape of the whiskers meant that the tip of the whisker was much smaller than that of the base, as shown in Fig. 3. The ratio of tip to base of this sample whisker α is about 1–10 and the shape of whisker α can be approximately fitted by an exponential function.

3.2. Effect of controlled loading modes

To carry out indentation tests, one can choose either to control indentation depth or indentation force. As an example, Fig. 4a and b shows the typical load–depth curve of whisker B3 from nanoindentation tests by two controlled loading modes, respectively. A constant depth rate of 100 nm/s and a constant load rate of 0.1 mN/s with a holding time of 5 s were adopted to eliminate the so-called "nose effect" for most biomaterials [21] whereby, without a holding time at peak load, an overhanging portion (just like a nose) would appear in the initial portion of unloading curve due to creep effect. This results in a negative slope and makes it impossible to employ the Oliver–Pharr method to calculate the indentation modulus.

In our tests, load relaxation can be observed during the holding period as increasing penetration depth over time under depth controlled mode (see Fig. 4a), and creeping occurs under load controlled mode (see Fig. 4b), both of which are typical phenomena

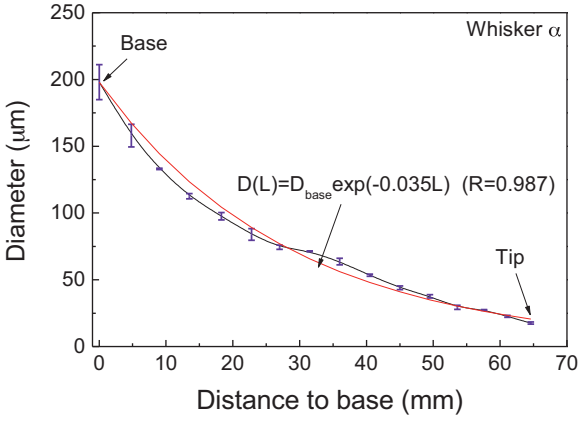

Fig. 3. The diameter of whisker α along the axis.

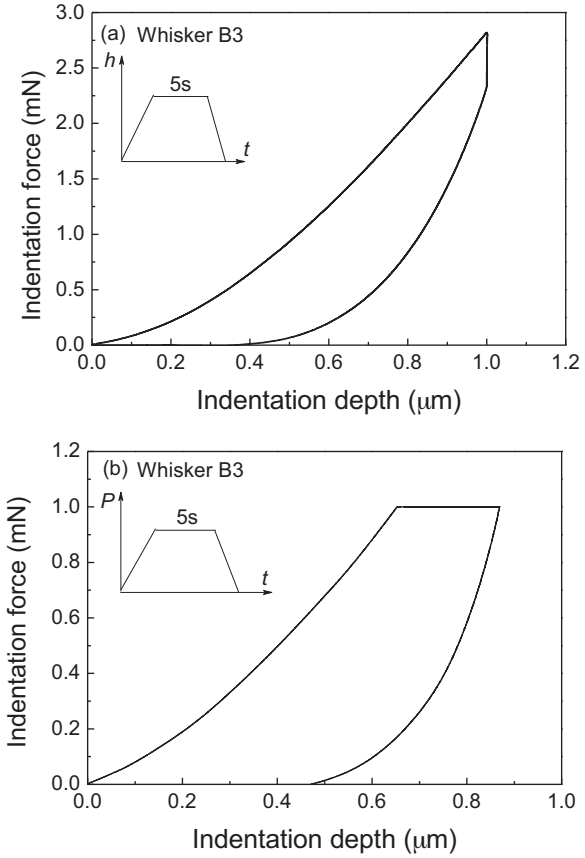

Fig. 4. Typical nanoindentation load–depth curves of whisker B3 with (a) depth controlled mode and (b) load controlled mode.

for visco-elastic materials. Following the Oliver–Pharr method presented in Section 2.3, it is found that indentation moduli for whisker B3 are almost the same for the two controlled modes with a difference of about 5%. In practice, indentation force can be greatly different at a same indentation depth for different whiskers and it is difficult to apply a reasonable indentation force to avoid the indentation depth being too small or too large. Therefore, depth-controlled mode was applied in the following indentation tests of whiskers.

3.3. Effect of holding time and loading rate

Many tissues, especially hydrated soft tissues, exhibit time-dependent behavior under physiological conditions [21,24]. The most readily observed effect of viscoelasticity on indentation is creeping at constant load with different holding times. Fig. 5a indicates that holding time affects the indentation modulus of whisker B4. As holding time varied from 2 s to 80 s with a fixed loading rate 0.1 mN/s, the indentation modulus decreased from 2.34 ± 0.34 GPa to 2.14 ± 0.03 GPa. The indentation modulus approached a steady value when the holding time was longer than 20 s. A similar effect of a stable indentation modulus has also been observed after a load holding period of 60 s in regenerating long bones [25]. Using a fixed hold time of 2 s, we investigated the influence of loading rate on indentation modulus. Fig. 5b shows that the indentation modulus slightly increased from 1.93 ± 0.15 GPa to 2.17 ± 0.53 GPa with increased loading rate and a stable modulus value was obtained at loading rate over 1 mN/s. Such visco-elastic behavior of rat whisker poses interesting questions for their normal function in the awake behaving animal and we plan to study this behavior in future experiments by using Nanoscale Dynamic

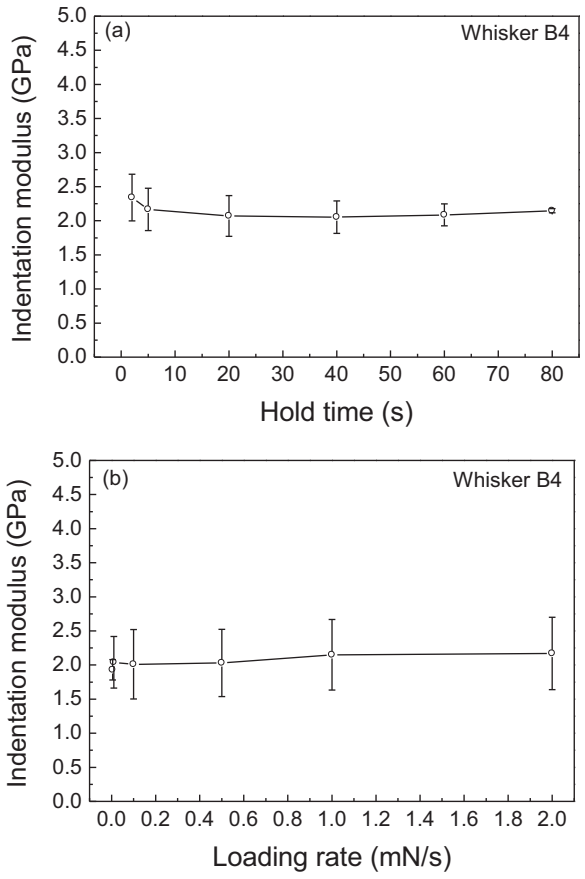

Fig. 5. Indentation modulus of whisker B4 (a) with different holding times and a fixed loading rate of 0.1 mN/s and (b) with different loading rates and a fixed holding time of 2 s.

Mechanical Analysis (NanoDMA) to measure the storage modulus and loss modulus of the rat whisker material.

3.4. Effect of indentation depth

For biomaterials, a decreased indentation modulus is observed with an increased indentation depth [16,26] due to visco-elasticity, surface roughness and size effects. The measured indentation moduli of whisker B3 from the indentation curves at different depths are presented in Fig. 6 where it can be seen that indentation modulus and standard derivation exhibit obvious depth-dependence and decrease with increased indentation depth.

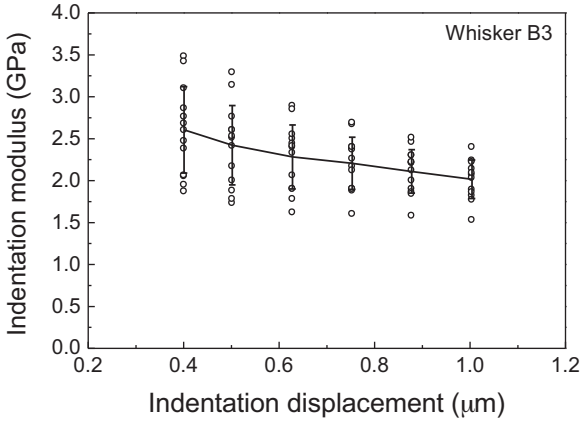

Fig. 6. Indentation modulus of whisker B3 at different indentation depths.

Surface roughness will increase the standard deviation with decreasing indentation depth. Moreover, visco-elasticity and size effect will decrease the indentation modulus with increasing indentation depth. In practice, it is unknown what is the most suitable indentation depth for measuring the depth-dependent indentation modulus. Hence, an average indentation modulus at different depths becomes a good choice, and was applied in our study to report the modulus results in the following sections.

3.5. Effect of tissue freshness

Test condition has been shown to be an important factor for biomaterials: the elastic moduli of the wing membranes are 2.85 ± 0.23 GPa and 2.74 ± 0.28 GPa for living and dead dragonflies [14], respectively. Similarly, the dry mature human enamel has a larger elastic modulus than a fresh one [27]. Given that the most hydrated soft tissues will become "harder" with decreased moisture content [28] and this could affect our measurements, we investigated the effect of freshness on indentation modulus of the rat whisker. The indentation tests were carried out on the same whisker sample C3 24 h and two weeks after detachment from the rat, as shown in Fig. 7. The measured indentation modulus of C3 is 1.71 ± 0.32 GPa after 24 h detachment and 1.74 ± 0.43 GPa after two weeks detachment. These results mean that there is only about 1.8% difference of the measured modulus between the two test conditions, indicating that the test time has no obvious influence on the indentation modulus of whisker C3, in line with the wing membranes of dragonfly (about 3.9% difference in elastic modulus for living and dead samples) [14]. A possible reason why the whiskers appeared to be resistant to drying-out effects may be that moisture is only supplied by the medulla cavity of rat whisker. The medulla layer is in the center of the whisker and only takes up about 11.3% of the external diameter. The outside layer of the whisker is the compact cuticle [15], which makes the hydrate not easy to lose even if the whisker has been long exposed in air.

3.6. Indentation moduli for all the whiskers

Combining the above discussion, indentation tests were performed to measure the indentation modulus of the 24 major whiskers. A typical discrimination process, such as whisker sweeping against or tapping an object, normally lasts for a very short time. Therefore, for the rat whisker material with a viscoelastic behavior, the measured indentation modulus with a short holding time at the peak load is more useful for studying the mechanical behavior of the rat whisker sensor. Consequently, the holding time was selected as 2 s. Additionally, we used the

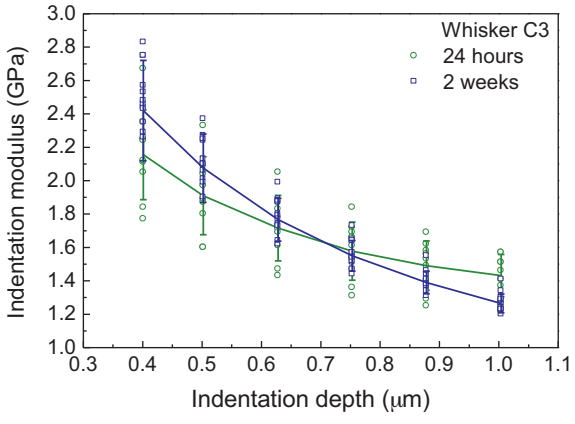

Fig. 7. Indentation modulus of whisker C3 at different test times after detached from the rat.

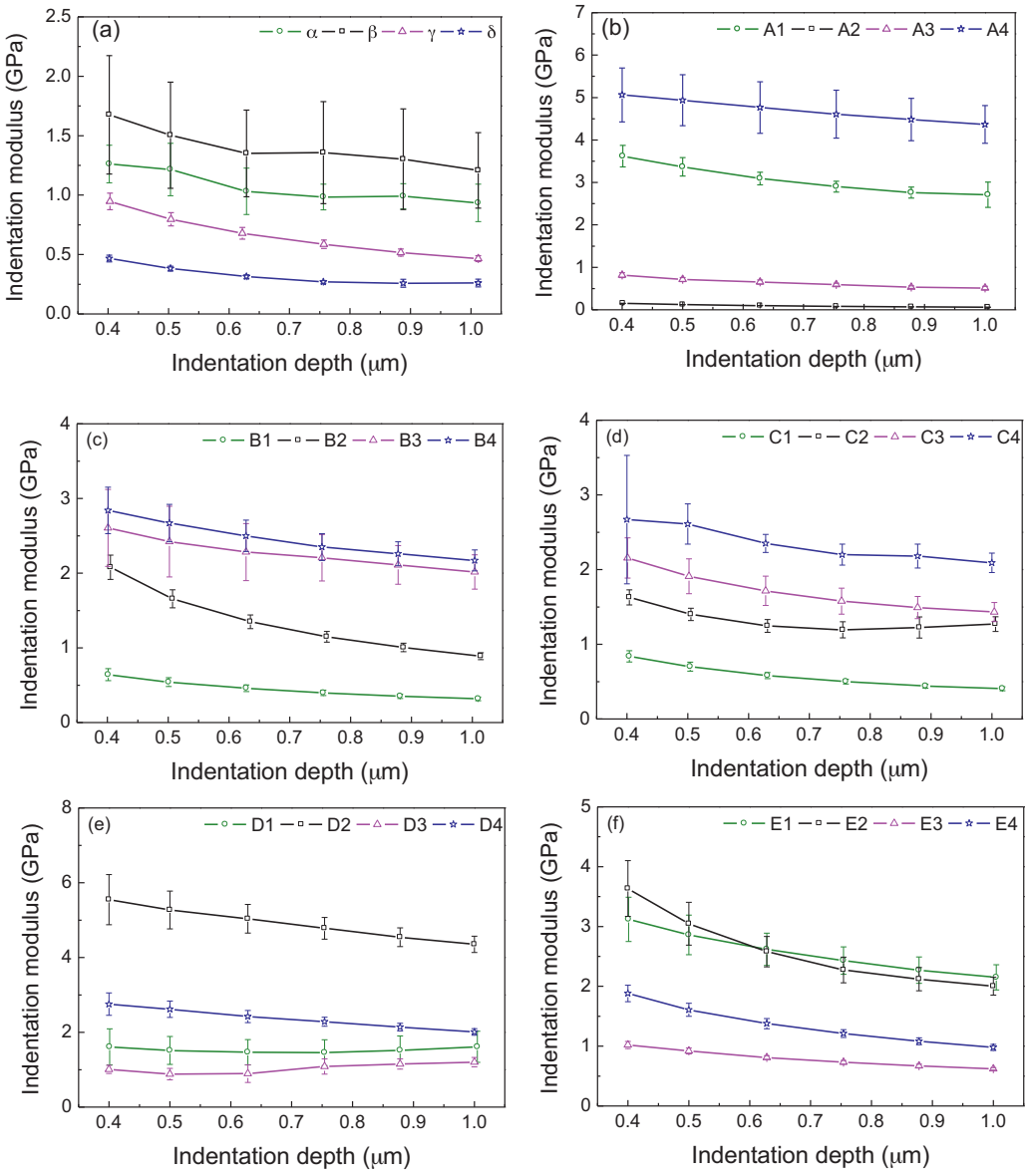

Fig. 8. Depth-dependent indentation modulus for the 24 major whiskers: (a) α, β, γ, δ; (b) A1–A4; (c) B1–B4; (d) C1–C4; (e) D1–D4; and (f) E1–E4.

depth-controlled mode with a displacement rate of 100 nm/s as a reasonable loading condition. The curves of indentation modulus versus indentation depth are shown in Fig. 8 where all data are presented as mean value ± standard deviation.

It was found that the indentation modulus and its standard deviation exhibit a depth-dependence. Except for whisker D3, for all other whiskers, the indentation modulus remarkably deceases with an increased indentation depth. Indentation moduli for the 24 major whiskers are summarized in Table 2. Table 2 shows that the average indentation modulus for each whisker varies from 0.33 ± 0.08 GPa (for whisker δ) to 4.92 ± 0.58 GPa (for whisker D2). Whiskers in the same arc (i.e., in the same caudal position on the face and therefore with similar length and diameter) have different indentation moduli, e.g., α, β, γ, δ whiskers have indentation moduli of 1.09 ± 0.2 GPa, 1.40 ± 0.41 GPa, 0.67 ± 0.17 GPa, 0.33 ± 0.08 GPa, respectively. This makes it clear that the length and diameter of whiskers had no direct relationship to indentation modulus, e.g., whisker δ has a larger length and diameter but the smallest indentation modulus.

Some similar biomaterials were also investigated by nanoindentation measurements or situ tensile testing. The elastic modulus is 2.25–2.5 GPa for hair from a horse's mane [29], 1.19–1.25 GPa for merino wool [30] and 3.3 GPa for hair of human [31], which is closed to the values of rat whisker. The Palmetto wood microfiber deviate significantly from the trend with an average reduced modulus of 11.44 GPa [32].

It is noted that the bending and rotational stiffness are two important parameters for studying the mechanical behavior of rat whiskers. If a whisker with length L is modeled as a straight cantilever beam with a conical shape rotating against a motionless object, the bending stiffness M at distance x from the whisker base can be calculated as

$$M(x) = \frac{1}{64}\pi E D_{base}^4 \left(1 - \frac{x}{L}\right)^4 \tag{3}$$

where D_{base} is the diameter of the whisker cross-section at the base and E is the elastic modulus. Under the assumption of small deformation and small rotation, the rotational stiffness K of an elastic conical beam is defined as $dM/d\theta$ (θ is the deflection angle) and it can be calculated as [6]

$$K(x) = \frac{3}{64}\pi E D_{base}^4 \left(\frac{1}{x} - \frac{1}{L}\right) \tag{4}$$

Assuming the Poisson's ratio ν being 0.4 and applying the measured indentation modulus to Eq. (3) ($E = E_r(1-\nu^2)$), the bending stiffness at the base of a whisker is predicted within the range of 0.58–134.79 mN mm^2, see Table 2. The rotational stiffness at the middle of a whisker is within 0.06–10.93 mN mm/rad according to Eq. (4) as, see Table 2. It has found a large difference in bending and rotational stiffness for different whiskers. This implies that different whiskers have different resistant capacities to bending and rotation loadings. As a whole, whiskers α, β, γ, δ and the first two of each row have larger bending and rotational stiffness. These results can be used to study the mechanical behavior of the rat whisker sensor system or a biomimetic sensor.

4. Conclusions

The nanoindentation technique was performed to investigate the indentation modulus of rat whisker. The findings are summarized as follows:

(1) The depth controlled mode and load controlled mode do not display a significant difference in indentation modulus. It is found that rat whisker exhibits obvious visco-elastic characteristic, load relaxation effect can be observed under displacement controlled mode and creeping effect occurs under load controlled mode.
(2) The indentation modulus decreases with an increased holding time and a decreased loading rate. It approaches a stable value when the holding time is over 20 s or the loading rate is over 1 mN/s.
(3) The indentation modulus of rat whisker exhibits obvious depth-dependence: it decreases with increased indentation depth. The influence of tissue freshness is negligibly small.
(4) The length and diameter of whiskers had no direct relationship to the indentation modulus at the base.
(5) The average indentation moduli of 24 major rat whiskers were reported to range from 0.33 GPa to 4.92 GPa. Moreover, the bending stiffness at base of whisker was evaluated within 0.58–134.79 mN mm^2 and the rotational stiffness at the middle of whisker was within 0.06–10.93 mN mm/rad.

Acknowledgments

This work was supported by National Natural Science Foundation of China (11025210 and 11202171) and the Fundamental Research Funds for the Central Universities (SWJTU12CX044). The experimental tests were carried out during QHK's academic visit to Monash University with the financial support from the Australian Government's Endeavor Awards program under the scheme of Endeavor Research Fellowships.

References

[1] J. Hipp, E. Arabzadeh, E. Zorzin, J. Conradt, C. Kayser, Methew E. Damond, P. König, J. Neurophysiol. 95 (2006) 1792–1799.
[2] S.P. Jadhav, D.E. Feldman, Curr. Opin. Neurobiol. 20 (2010) 313–318.
[3] J.A. Birdwell, J.H. Solomon, M. Thajchayapong, M.A. Taylor, M. Cheely, R.B. Towal, J. Conradt, M.J. Hartmann, J. Neurophysiol. 98 (2007) 2439–2455.
[4] J.H. Solomon, M.J.Z. Hartmann, Philos. Trans. R. Soc. B 366 (2011) 3049–3057.
[5] E.M. Staudacher, M. Gebhardt, V. Durr, Adv. Insect Physiol. 32 (2005) 49–205.
[6] J.H. Solomon, M.J.Z. Hartmann, Nature 443 (2006) 525.
[7] M.J.Z. Hartmann, N.J. Johnson, R.B. Towal, C. Assad, J. Neurosci. 23 (2003) 6510–6519.
[8] M.A. Neimark, M.L. Andermann, J.J. Hopfield, C.I. Moore, J. Neurosci. 23 (2003) 6499–6509.
[9] K. Carl, W. Hild, J. Mämpel, C. Schilling, R. Uhlig, H. Witte, Sens. J. IEEE 99 (2011) 1–7.
[10] B.W. Quist, R.A. Faruqi, M.Z. Hartmann, J. Biomech. 44 (2011) 2775–2781.
[11] D. Ziskind, M. Hasday, R. Sidney, H. Cohen, D. Wagner, J. Struct. Biol. 174 (2011) 23–30.
[12] V.T. Nayar, J.D. Weiland, A.M. Hodge, Mater. Sci. Eng. C 31 (2011) 796–800.
[13] P.K. Zysset, X.E. Guo, C.E. Hoffler, K.E. Moore, S.A. Goldstein, J. Biomech. 32 (1999) 1005–1012.
[14] F. Song, K.W. Xiao, K. Bai, Y.L. Bai, Mater. Sci. Eng. A 457 (2007) 254–260.
[15] E.K. Herzog, D.F. Bahr, C.D. Richards, R.F. Richards, D.M. Rector, Mater. Res. Soc. (2005) R3.6.1–R3.6.5.
[16] E. Donnelly, S.P. Baker, A.L. Boskey, M.C.H. van der Meulen, J. Biomed. Mater. Res. 77A (2) (2006) 426–435.
[17] S. Habelitz, S.J. Marshall, G.W. Marshall, Arch. Oral Biol. 46 (2001) 173–183.
[18] D. Voges, K. Carl, G.J. Klauer, R. Uhlig, C. Schilling, C. Behn, H. Witte, Sensors 4718 (2010) 1–7.
[19] T.Y. Tsui, G.M. Pharr, J. Mater. Res. 14 (1999) 292–301.
[20] Y. Cao, D. Yang, W. Soboyejoy, J. Mater. Res. 20 (2005) 2004–2011.
[21] D.M. Ebenstein, L.A. Pruitt, Nanotoday 1 (2006) 26–33.
[22] M.R. Vanlandingham, J.S. Villarrubia, Macromol. Symp. 167 (2001) 15–44.
[23] W.C. Oliver, G.M. Pharr, J. Mater. Res. 7 (1992) 1564–1583.
[24] Z.H. Wu, T.A. Baker, T.C. Ovaert, G.L. Niebur, J. Biomech. 44 (2011) 1066–1072.
[25] T. Ishimoto, T. Nakano, M. Yamamoto, Y. Tabata, J. Mater. Sci. Mater. Med. 22 (2011) 969–976.
[26] S. hengsberger, A. Kulik, P.H. Zysset, Bone 30 (2002) 178–184.
[27] L.H. He, M.V. Swain, Biomaterials 28 (2007) 4512–4520.
[28] A.J. Bushby, V.L. Ferguson, A. Boyde, J. Mater. Res. 19 (2004) 24–259.
[29] M. Kania, D. Mikolajewska, K. Marycz, M. Kobielarz, Acta Bioeng. Biomech. 11 (2009) 53–57.
[30] C.T. Gibson, S. Myhra, G.S. Waston, M.G. Huson, D.K. Pham, P.S. Turner, Text. Res. J. 71 (2001) 573–581.
[31] I.P. Sehadri, B. Bhushan, Acta Mater. 56 (2008) 774–781.
[32] A.L. Gershon, H.A. Bruck, S.W. Xu, M.A. Sutton, V. Tiwari, Mater. Sci. Eng. C 30 (2010) 235–244.